Magn Reson Mater Phy (2006) 19: 187–195
DOI 10.1007/s10334-006-0046-y

RESEARCH ARTICLE

Alex Frydrychowicz
Thorsten A. Bley
Jan T. Winterer
Andreas Harloff
Mathias Langer
Jürgen Hennig
Michael Markl

Accelerated time-resolved 3D contrast-enhanced MR angiography at 3T: clinical experience in 31 patients

Received:18 April 2006
Accepted: 24 July 2006
Published online: 26 August 2006

A. Frydrychowicz (✉) · T. A. Bley
J. T. Winterer · M. Langer
J. Hennig · M. Markl
Department of Diagnostic Radiology
and Medical Physics, University Hospital
Freiburg, Hugstetter Str. 55,
79106 Freiburg, Germany
Tel.: +49-761-2703802
Fax: +49-761-2703842
E-mail:
alex.frydrychowicz@uniklinik-freiburg.de

A. Harloff
Department of Neurology and Clinical
Neurophysiology, University Hospital
Freiburg, Breisacher Str.64, 79106
Freiburg, Germany

Abstract *Purpose*: To evaluate whether time-resolved 3D MR-angiography at 3T with a net acceleration factor of eight is applicable in clinical routine and to evaluate whether good image quality and a low artifact level can be achieved with a temporal update rate that allows for additional information on pathologies.
Materials and methods: Thirty-one consecutive patients underwent time-resolved 3D contrast-enhanced MR-angiography on a 3T system. Imaging consisted of accelerated 3D gradient echo sequences combining parallel imaging with an acceleration factor of four, partial Fourier acquisition along phase and slice encoding direction, and twofold temporal acceleration using view sharing. Data volumes representing the arterial and venous contrast phases were independently evaluated by two experienced radiologists by grading of image quality and artifact level on a 0–3 scale.
Results: Time-resolved MR-angiography was successfully performed in all subjects without the need for contrast agent bolus timing. Excellent arterial (average score = 2.65 ± 0.32) and good venous (average score = 2.56 ± 0.28) diagnostic image quality and little image degrading due to artifacts (average score = 2.20 ± 0.16) were confirmed by both independent readers (agreement in 65.2% of all evaluations). In 14 patients vascular pathologies were identified in the arterial phases. In eight examinations temporal resolution and depiction of contrast agent dynamics provided additional information about pathology.
Discussion: Without the necessity for additional bolus timing, time-resolved 3D contrast-enhanced MR-angiography with imaging acceleration along both the spatial encoding direction and temporal domain revealed excellent diagnostic image quality in neurovascular and thoracic imaging. Despite the limited spatial resolution as compared to high-resolution imaging of the carotid artery bifurcation, the results demonstrate the applicability of contrast-enhanced MR-angiography in thoracic and abdominal MRA as well as cervical imaging with a temporal update rate allowing for additional information on pathologies. Future studies may include an evaluation of optimal trade-offs between spatial and temporal resolution, different acceleration factors and a comparison to the gold-standard for accuracy.

Keywords Magnetic resonance angiography · Cardiovascular system · Arteries · Thoracic arteries · Veins · 3T

Introduction

The importance of contrast-enhanced 3D MR-angiography (CE-MRA) for the assessment of arterial vessels and pathologies has steadily increased over the last decade [1]. Moreover, recent technical and methodological advances have greatly enhanced scan performance and image quality [2–7]. Higher magnetic fields and the associated gain in SNR as well as effects on T1-relaxation [8,9] are highly beneficial for CE-MRA. Also, recently developed state-of-the-art data acquisition techniques, such as parallel imaging with generalized auto-calibrating partially parallel acquisitions (GRAPPA) [10], view sharing such as time-resolved echo-shared angiography technique (TREAT) or time-resolved imaging of contrast kinetics (TRICKS) [7,11,12] and partial Fourier acquisition in phase and slice encoding directions [13] have improved current imaging modalities. In combination with modern multi-channel systems, whole-body CE-MRA has become feasible [14,15]. Also, time-resolved acquisition of 3D volumes of arterial or venous regions of interest can be achieved [2,16–19]. With sufficient temporal resolution, the need for additional measurements and scan timing for optimal bolus timing is reduced. Furthermore, the reconstruction of separate arterial and venous phases of the contrast agent passage has the potential to minimize venous overlay. Additional information from temporal assessment of the distribution of contrast agent and the differences in tissue contrast enhancement may be useful for further diagnostic purposes.

Previous reports on 3D time-resolved CE-MRA focus on the pulmonary or renal vasculature or on neurovascular imaging at 1.5 T [7,19–25] and at 3 T [26]. Therefore, this study aims to evaluate whether time-resolved 3D MR-angiography at 3 T with a net acceleration factor of eight is applicable in clinical routine in different anatomical regions. A focus has been to evaluate whether the imaging protocol ensures good image quality and low artifact level with a temporal update rate that allows for additional information on pathologies.

Materials and methods

Human subjects

Thirty-one consecutive patients, 12 male, 19 female, age 60.7 ± 16.3 years (range 13–86 years) with a body weight of 73.9 ± 15.1 kg (range 48–109 kg) were included in our study. All patients were scheduled for regular CE-MRA for either exclusion or diagnosis of arterial pathologies in different regions of interest. Written informed consent was obtained from all patients. The study was approved by the local ethics committee.

Twelve patients were examined with a neurovascular coil for display of both the supraaortic branches and the arteries forming the circle of willis. Nineteen patients underwent CE-MRA with a body array coil to display the (1) thoracic arteries including the aorta, the proximal supraaortic branches and the subclavian artery or (2) the abdominal aorta including the proximal abdominal branches such as the celiac trunk, the mesenteric arteries and the aortic bifurcation. In a single experiment (3) the superficial artery was examined as a chronic occlusion needed to be evaluated before surgery (see also Table 1 for patients with pathologies detected in the arterial system).

MR-imaging

All examinations were performed on a 3T system (Magnetom TRIO, Siemens Medical Solutions, Erlangen, Germany, maximum gradient strength = 40 mT/m, rise time = 200 μs).

Image acquisition consisted of a rf-spoiled gradient echo sequence with a flip angle of $11 - 23°$ [depending on patient weight and associated specific absorption rate (SAR) limitations]. In order to permit data acquisition with an acceptable spatial resolution as well as temporal update rate of the order of 2.0–3.5 s, several image acceleration procedures were combined in order to generate an useful time-resolved 3D CE-MRA protocol for neurovascular imaging (cranial and cervical vessels) as well as the depiction of the thoracic angiography (thoracic aorta and branching vessels).

For all acquisitions, an eight-channel receiver coil was utilized for parallel imaging (k-space based GRAPPA reconstruction) with an acceleration factor of four along the phase encoding direction and 32 reference lines [10,27]. In addition, partial Fourier acquisition was used along the phase and slice encoding direction (for both, partial Fourier factor = 6/8). Further, a recently

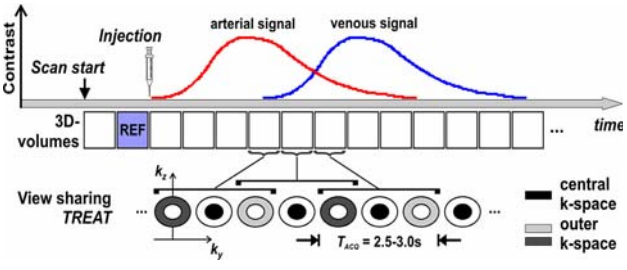

Fig. 1 Schematic illustration of the data acquisition and image acceleration strategies used for time-resolved CE-MRA. Contrast agent administration (*Injection*) was started following the acquisition of two pre-contrast 3D data sets. A series of successively acquired 3D volumes covered the arterial and venous filling phases of the contrast agent. The effective temporal update rate was accelerated using view sharing in the ky–kz space as exemplary illustrated for three successive time frames. The data set used for background subtraction is indicated by *REF*

reported view sharing strategy along the temporal domain (TREAT imaging, see also Fig. 1) based on elliptical centric view ordering [4, 5], double update rate of central k-space and sharing of outer k-space regions was employed. As a result, effective temporal resolution was improved by a factor of one-third without compromising the spatial resolution of the individual 3D data volumes [12].

With the resulting imaging protocol, 20–30 T1-contrast 3D data volumes were acquired consecutively with a temporal update rate of 2.5–3.3 s. CE-MRA was performed using intravenous gadolinium contrast agent (Gadobenate dimeglumine, Gd-BOPTA chelate, Multihance, ALTANA Pharma, Konstanz, Germany, molar concentration 0.5 M, single dose = 0.1 mmol/kg body weight, injection rate = 3–4 ml/s). The injection duration was variable with respect to the individual patient's body weight. As a result of the high temporal update rate (≤ 3.3 s) no individual assessment of bolus arrival time was needed and contrast agent injection was started after the completion of the acquisition of the first two 3D data volumes (approximately 6 s following the initiation of data acquisition). To avoid transient effects, the second data volume was used as a full-resolution pre-contrast data set for background signal elimination through mask subtraction. For a schematic illustration of scan and injection timing see Fig. 1.

In 12 patients neurovascular CE-MRA was performed using a eight-channel phased array neurovascular coil, which permitted full coverage of the aortic arch, the supra-aortic vessels, neck and the entire head. 3D MRA data were acquired in a coronal volume with a temporal and spatial resolution of 2.94 ± 0.17 s and $1.74 - 1.94 \times 1.04 \times 1.5\,\text{mm}^3$, respectively. Further pulse sequence parameters were as follows: $\text{TE} = 0.87 - 1.02$ ms, $\text{TR} = 2.1 - 2.39$ ms, $\text{FOV} = (300 - 400 \times 400)\,\text{mm}^2$. In the majority of cases, a slab thickness = 120 mm, and 80 slices/slab were acquired with acquisition matrix = 288×384. In cases where the image parameters had to be adapted due to the patients' individual anatomy, the slice thickness was 1.2 mm in one case and in two cases 2.1 and 2.5 mm, respectively.

For 19 patients time-resolved thoracic 3D MRA examinations were executed using an eight-channel phased array body coil. The coil was carefully positioned to cover either the entire thoracic aorta including the proximal supra-aortic vessels or the abdominal aorta with a spatial resolution of $1.83 - 2.38 \times 1.25 \times 1.5\,\text{mm}^3$. In a single experiment, the superficial femoral artery was depicted. The temporal resolution in all examinations with the body array coil was 2.72 ± 0.15 s.

Further pulse sequence parameters were as follows: $\text{TE} = 0.78 - 0.88$ ms, $\text{TR} = 1.97 - 2.15$ ms, $\text{FOV} = (280 - 400 \times 400)\,\text{mm}^2$, acquisition matrix = $224 - 320 \times 384$. As with the neurovascular coil, the majority of examinations were performed with slab thickness = 120 mm, with 80 slices/slab. Depending on the coil and volume coverage either a coronal or sagittal volume was acquired. In three patients, the slice thickness was 2 mm in order to adapt the acquired volume to the patient's individual anatomy.

Image reconstruction

Maximum intensity projections (MIP) of each time-resolved data volume performed on a Siemens WIZARD system (Siemens Medical Solutions, Erlangen, Germany). For complete appreciation of the 4D nature of the data, an additional software package (Acquarius Server/NetClient Visualization software solution, TeraRecon Inc., San Mateo, CA, USA) was used for interactive 3D rotation of data sets and inspection from user selected view angles 3D diagnostic evaluation of the data. In addition, the entire data set was exported as a rotation time-resolved 3D MIP animation in movie format.

Image interpretation and statistical analysis

All data were evaluated by two independent radiologists with at least 5 years of experience in cardiovascular MR imaging. Readers were blinded to the patients' clinical background and to the other reader's results. For the interpretation of the data, non-subtracted and subtracted images of all time frames, maximum intensity projections (MIP) as well as a rotating time-resolved 3D MIP animation were assessed for all patients. In some cases, multi-planar reconstructions (MPR) were used to further evaluate findings.

Semi-quantitative image grading was performed in time frames with maximum arterial and venous signal intensities, respectively. A grading scale with 0 = poor diagnostic quality, no diagnosis possible; 1 = moderate diagnostic quality, diagnosis hampered but possible; 2 = good diagnostic quality, diagnosis possible; and 3 = excellent diagnostic quality, diagnosis possible, was applied to three arterial and venous regions: aorta or caval vein, 1st arterial or venous branch (e.g., common carotid artery or internal jugular vein) and 2nd arterial or venous branch (e.g., internal carotid artery or sinus veins). In case of a different location of the arterial region of interest (abdomen, thigh), corresponding 1st and 2nd branch arteries and veins were used for evaluation.

Since parallel imaging and free breathing can degrade image quality, a grading of the severity of related artifacts (blurring, ghosting and fold-over artifacts) with respect to the diagnostic image quality was performed. The grading was performed using 0 = severe artifacts, no diagnosis possible; 1 = moderate artifacts, diagnosis hampered but possible; 2 = minor artifacts, diagnosis possible; and 3 = no artifacts, diagnosis possible.

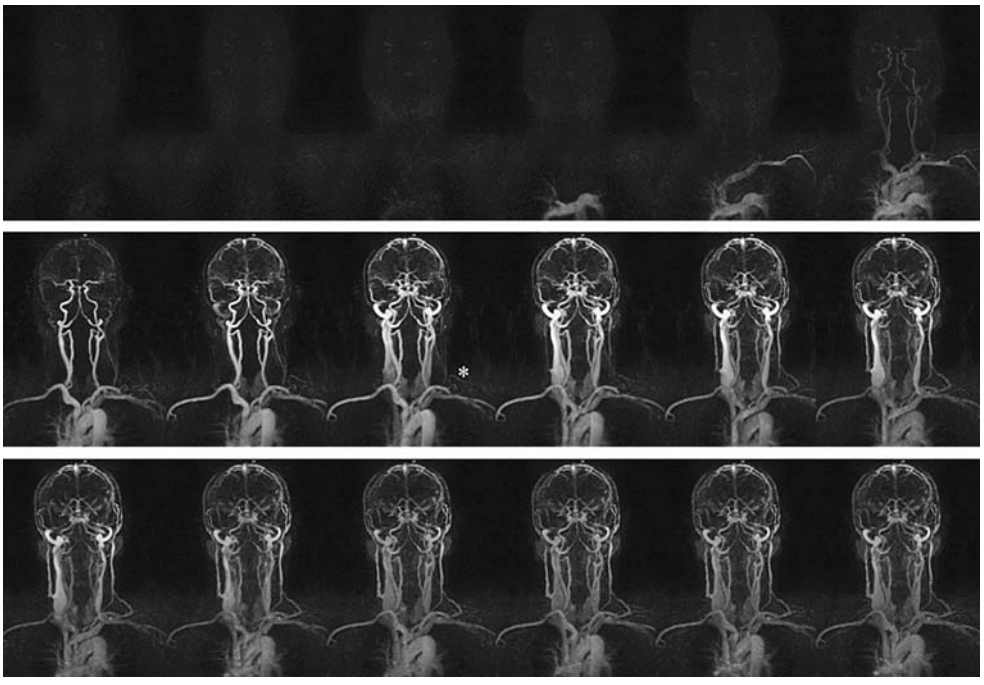

Fig. 2 Time series (*top left to lower right*) of maximum intensity projections (MIP) of a time-resolved CE-MRA in a patient (patient number 31, see Table 1) with a stenosis of the left subclavian artery (*asterisk*). Dynamics of the contrast agent passage as well as clear delineation of arterial and venous vasculature can clearly be idenfied

Finally, all three image characteristics (i.e., arterial and venous image grading and image quality degradation due to artifact generation) were summarized in a mean 0–3 score rating overall arterial or venous diagnostic image quality and artifact level (see Tables 2 and 3).

If a pathology was detected, the type of pathology and its location was reported (e.g., stenosis >50%, aneurysm >25% of age-related vascular lumen diameter, plaque). Further, the information whether useful additional information beyond that contained in a single, non-time-resolved 3D data set was collected.

All results are given as mean ± standard deviation.

Results

Time-resolved 3D CE-MRA was successfully performed in all human subjects. All acquisitions were performed during free breathing, acquiring 20–30 (21.97 ± 2.46) consecutive 3D data volumes. The total scan time for all MR angiographies was between 50 and 90 s. Mean temporal resolution was 21.5 ± 1.4 acquisitions per minute (range 23.8 and 18.3, frame rate 2.5–3.3 s). Both time to peak arterial and venous contrast demonstrated wide ranges of 13.1–36.4 s (arterial, mean 24.0 ± 5.3 s) and 26.2–52.2 s (venous, mean 36.5 ± 6.2 s), respectively. Nevertheless, arteries and veins were clearly distinguishable in each patient underlining the robustness of our time-resolved imaging protocol.

An example of image quality and dynamics of contrast agent passage is illustrated in Fig. 2 which shows a series of time-resolved MIP images of the cervical and cranial arteries in a patient with a stenosis of the left subclavian artery.

Grading of arterial and venous image quality and influence of artifact level on diagnostic image quality is summarized in Tables 2 and 3. Table 2 lists the mean image quality and artifact presence as well as the related total image score for each reader. Both readers attested overall good to excellent image quality for all arterial and venous segments. In total, data analysis revealed excellent arterial image quality (mean $= 2.65 \pm 0.32$, reviewer1(R1) : 2.56 ± 0.38 and reviewer 2 (R2): 2.73 ± 0.37) and good venous image quality (mean $= 2.56 \pm 0.28$, R1 : 2.46 ± 0.39, R2 : 2.66 ± 0.36). The generation of artifacts did not hamper diagnostic image quality (mean $= 2.20 \pm 0.16$, R1 : 2.18 ± 0.28, R2 : 2.23 ± 0.18). Although some blurring and ghosting from respiration and/or pulsatile flow was observed in most images, influence of artifacts on diagnostic image quality was on average still rated as minor. Taking into account only those measurements where pathologies were detected, resulting values were only slightly altered with excellent arterial image quality (mean 2.56 ± 0.35, R1 : 2.45 ± 0.42, R2 : 2.67 ± 0.43) and good venous

Table 1 Patients with patholgies

No.	Sex	Age (years)	BW (kg)	Coil	Finding	Additional information by 4D
4	Female	70	80	NV	Stenosis right ICA and ECA	Late inflow on right supraaortic branches
7	Female	25	48	BA	Stenosis prox. right subclavian artery	No subclavian steal, good delineation of collateral arteries
8	Male	63	85	NV	Kinking right subclavian artery	None
10	Female	70	66	BA	Bypass AAo to right CCA	Filling of right subclavian by retrograde filling of right CCA
11	Female	36	92	BA	Aortic coarctation A. lusoria Bypass AAo to DAo	None
12	Male	40	78	BA	Type B dissection Multiple aneurysms	Early filling of true lumen
14	Male	82	83	BA	Occlusion right SFA Stenosis left SFA	Good discrimination of collaterals and venous return
16	Male	13	48	BA	Stenosis DAo Prominent intercostal arteries	None
19	Male	69	58	BA	Plaque DAo	None
20	Male	60	100	BA	Occlusion left ECA	None
21	Female	53	72	BA	Kinking of left vertebral artery	None
22	Female	71	75	BA	Stenosis brachiocephalic trunc Plaque aortic arch and DAo	None
25	Male	50	109	BA	Type A dissection Prosthesis AAo Aneurysms DAo	True lumen filling first
28	Male	56	78	BA	Plaque DAo	None
29	Female	78	60	BA	Plaque DAo	None
30	Male	52	72	BA	Type B dissection Aneurysm thoraco-abdominal stent celiac trunc and sup. mesenteric artery	None
31	Female	79	55	NV	Stenosis left A. and V. subclavia	None

List of pathological findings in 31 consecutively examined patients
BA body array, *NV* neurovascular, *DAo* descending aorta, *AAo* ascending aorta, *CCA* common carotid artery, *ECA* external carotid artery, *ICA* internal carotid artery

image quality (mean = 2.45 ± .032, R1 : 2.26 ± 0.35, R2 : 2.64 ± 0.40). Consistent with results from all subjects, only minor influence of artifacts on diagnostic image quality (mean = 2.17 ± 0.13, R1 : 2.12 ± 0.29, R2 : 2.22 ± 0.20) was observed (see Table 3).

An agreement between both readers was achieved with identical gradings in 65.2% of all evaluations, 61.3% of the arterial, 60.7% of venous segments and 74.2% of all artifact level gradings). In all but two of the remaining gradings (in artifact level determination), both reviewer gradings differed by 1 (see Table 4). Three venous evaluations were not performed because the optimal venous contrast was not reached due to slow venous contrast agent travel times.

Vascular pathologies, as summarized in Table 1, were independently identified in 19 out of 31 patients by both readers. For eight pathologies, both radiologists agreed that additional information was provided by the temporal information and depiction of the dynamics of the contrast agent bolus passage. Four patients presented with large partially calcified plaques of the descending aorta. Stenoses and occlusions of the supra-aortic arteries were identified in six patients. In the remaining 12 patients, both readers independently agreed on unsuspicious MR angiographic findings.

An example for the additional value of temporal information on contrast agent dynamics is shown in Fig. 3 (patient 10) where time-resolved measurements aided the description of arterial blood supply to the right arm. After occlusion of the proximal brachiocephalic trunk, this 70-year-old female patient had received a bypass from the ascending aorta to the right carotid bulb. Excellent contrast of the arterial lumen and the filling of the bypass, followed by the retrograde filling of the common

Table 2 Image quality in all examinations

Arteries	Aorta	1st branch	2nd branch	Total
Reader 1	2.48 ± 0.51	2.61 ± 0.5	2.58 ± 0.67	2.56 ± 0.38
Reader 2	2.55 ± 0.51	2.81 ± 0.4	2.84 ± 0.37	2.73 ± 0.37
Veins	Vena cava	1st branch	2nd branch	Total
Reader 1	2.25 ± 0.44	2.57 ± 0.57	2.57 ± 0.57	2.46 ± 0.39
Reader 2	2.43 ± 0.5	2.71 ± 0.46	2.82 ± 0.39	2.66 ± 0.36
Artifacts	Blurring	Ghosting	Fold-over	Total
Reader 1	2.1 ± 0.54	1.97 ± 0.18	2.48 ± 0.57	2.18 ± 0.28
Reader 2	2.0 ± 0.26	2.0 ± 0.18	2.65 ± 0.49	2.23 ± 0.18

Image quality grading
Arteries/veins:
0 = poor image quality, non-diagnostic
1 = moderate image quality, diagnosis hampered
2 = good image quality, diagnosis not hampered
3 = excellent image quality
Artifacts:
0 = severe artifacts, no diagnosis possible
1 = moderate artifacts, diagnosis hampered
2 = minor artifacts, no influence on diagnosis
3 = no artifact presents
Total image quality score:
0 – 0.75 poor
0.76 – 1.5 moderate
1.51– 2.2 good
2.21 – 3 excellent

carotid artery (CCA) and the subclavian artery can clearly be appreciated. Image quality in this patient was graded excellent for arterial quality (total score R1: 2.6, R2: 3.0), excellent for venous quality (total score R1: 2.6, R2: 3.0) and good for artifact generation and influence on image quality (total score R1: 2.0, R2: 2.0).

In a 50-year-old male patient (patient 25) a regular follow-up MR-angiography after Type-A dissection and supra-coronal prosthesis implantation was performed (see Fig. 4). Next to a good contrast of the enlarged intravascular lumen a clear differentiation between true and false lumen of the dissected descending aorta was achieved. Slightly reduced grading of image quality (total score arterial: R1: 1.6, R2: 1.6; total score venous: R1: 1.3, R2: 2.0) and for artifact influence (total score R1: 2.0, R2: 2.3) did not hamper the identification of an aneurysm which has developed in the aortic arch. Table 1 also lists all remaining cases for which temporal resolution provided additional diagnostic information.

Table 3 Image quality in patients with pathologies

Arteries	Aorta	1st branch	2nd branch	Total
Reader 1	2.53 ± 0.51	2.56 ± 0.51	2.35 ± 0.79	2.45 ± 0.42
Reader 2	2.53 ± 0.51	2.71 ± 0.47	2.78 ± 0.44	2.67 ± 0.43
Veins	Vena cava	1st branch	2nd branch	Total
Reader 1	2.21 ± 0.43	2.50 ± 0.65	2.21 ± 0.58	2.26 ± 0.35
Reader 2	2.36 ± 0.5	2.64 ± 0.50	2.71 ± 0.47	2.64 ± 0.40
Artifacts	Blurring	Ghosting	Fold-over	Total
Reader 1	2.06 ± 0.43	1.94 ± 0.24	2.35 ± 0.61	2.12 ± 0.29
Reader 2	2.06 ± 0.24	2.06 ± 0.24	2.47 ± 0.51	2.22 ± 0.20

Discussion

In a series of 31 consecutive patients eightfold accelerated time-resolved 3D contrast-enhanced MR-angiography demonstrated to be a useful tool for the assessment of arterial and venous vasculature. The imaging protocol yielded good image quality in neurovascular and thoracic imaging if large fields of view are desired or time-resolved imaging is indicated. Run-off studies were not performed as this technical feature was not available on the scanner software. Results from image quality evaluations indicate that the temporal resolution <3.3 s used in this study yields good to excellent diagnostic image quality without the need for additional bolus timing assessment and can provide additional information. The herein used spatial resolution, however, cannot be compared to high resolution imaging e.g., of the carotid arteries or especially the carotid bifurcation but shows applicable if large fields of view are demanded for example for an angiographic overview.

Especially the wide range of arterial and venous contrast agent passage time as observed here points towards the utility of time-resolved imaging. Based on the combination of a fourfold acceleration by parallel imaging along the spatial encoding direction and twofold temporal acceleration, data could be acquired with a sufficiently high temporal update rate for the separation of arterial and

Table 4 Agrement of image quality grading

Grading differed by	Arterial phase	Venous phase[a]	Artifact level
0	61.3% (57)	60.7% (51)	74.2% (69)
1	48.7% (36)	39.3% (33)	23.7% (22)
2	0 (0)	0 (0)	2.1% (2)

This table lists the level of agreement between both blinded readers in relative and absolute numbers (in brackets)
[a]Please note that three venous ratings were not performed due to a delayed enhancement and consecutively diminished venous contrast enhancement

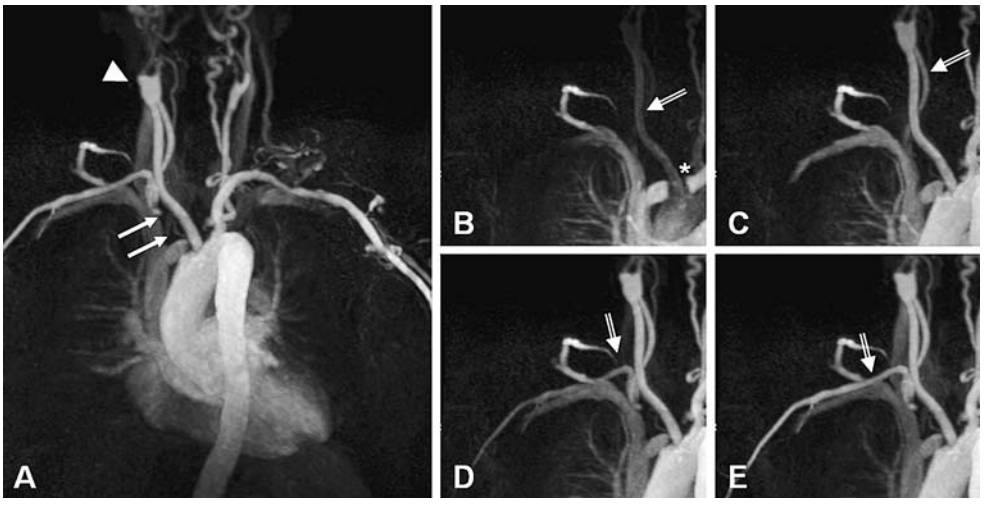

Fig. 3 Time-resolved CE-MRA in a 70-year-old female patient(patient number 10, see Table 1) after aorta-carotid bypass (*white arrows*) due to a proximal occlusion of the brachiocephalic trunk. Maximum intensity projections (MIP) at maximum arterial contrast (**a**) give an overview over the arterial vasculature. The distal anastomosis is discretely dilated (*arrowhead*). Additionally, time-resolved CE-MRA illustrates the blood flow distribution from the bypass to the anastomosis at the carotid bifurcation (**b, c**), a backward flow through the common carotid artery to the distal brachiocephalic trunk (**d**) and to the subclavian artery (**e**). The *asterisk* indicates the signal void due to suture material of the proximal bypass anastomosis

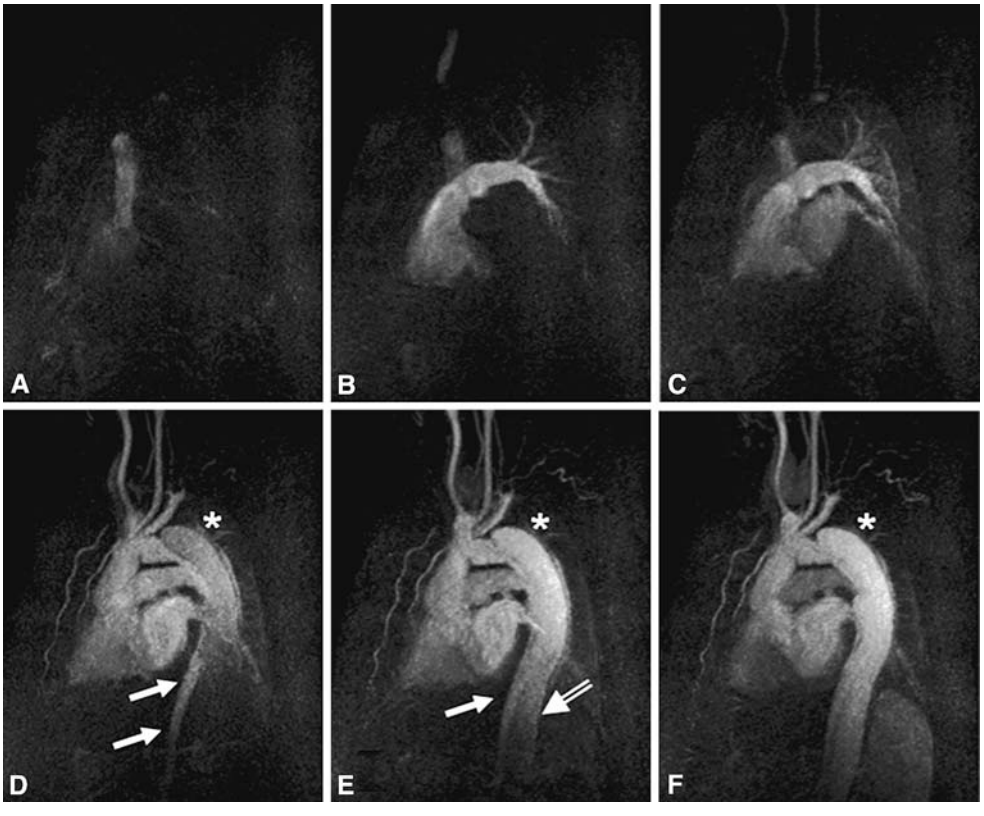

Fig. 4 Six of 20 time frames from time-resolved thoracic CE-MRA in a 50-year-old male patient (patient number 25, see Table 1) after Type-A dissection and implantation of a ascending aortic conduit. Early enhancement of the true lumen (*white arrows*) if compared to the false lumen (*open arrow*) can clearly be appreciated. Note the development of an aneurysm within the false lumen of the aortic arch (*asterisk*)

venous phase while maintaining a reasonably high spatial resolution in large field-of-view imaging within the individual 3D volumes. When starting the acquisitions prior to intravenous contrast administration, the venous bolus arrival, the arterial phase, and venous phase can sufficiently be distinguished. Despite application of the herein used accelerated imaging protocol with a net acceleration of eight, no severe image reconstruction artifacts were observed even on the non-subtracted source images. Further improvements of the measurement protocol could be achieved by integration of an acceleration along the slice encoding direction which is, however, currently not available on our MR scanner.

As presented in the clinical examples, contrast agent dynamics may offer additional diagnostic information such as the distribution of arterial supply to the region of interest after peripheral bypass surgery. Also, as seen in two patients in this study, the description of collaterals in the presence of chronic arterial occlusion is feasible in a single examination.

Potential drawbacks of the presented imaging protocol are related to the trade-off between temporal and spatial resolution and limitations with respect to the image evaluation strategy.

The focus of the presented study was to ensure good diagnostic image quality with a temporal resolution that also allows for additional information on pathologies and a clear separation of arterial and venous phase. Future studies are warranted for the evaluation and definition of optimized trade-off between spatial and temporal resolution adapted to individual applications.

Although the purpose of this study was the evaluation of diagnostic image quality of time resolved CE-MRA at 3T, no quantitative SNR or CNR calculations were performed. Such an evaluation would have been hampered by the non-uniform spatial distribution of noise associated with parallel imaging [28]. The spatially varying amplification of noise as characterized by the "g"-factor by Pruessmann et al. [29] is not trivial and specifically relevant in protocols using higher acceleration factors. Despite repetitive measurements at virtually the same anatomical position, all measurements were performed during free breathing which further hinders a reliable SNR estimation. Thus, characterization of image quality was based on a semi-quantitative evaluation by experienced radiologists.

The facilitated application of contrast media without the need for an optimal bolus timing may be especially important for pediatric patients with fast contrast media passage (e.g., patient 11), patients with impaired cardiac output, and patients with high dilution volumes (e.g., patients 25 and 30) such as aneurysms. Specific attention should be paid to examinations of children as the high demands in terms of spatial resolution may not be sufficiently addressed by our imaging protocol.

Since time-resolved CE-MRA at 3T is fast and easy to perform, it could easily be attached to virtually any contrast-enhanced MR imaging protocol in which vascular pathologies are of interest. In the presence of pathological findings, however, this application of well established CE-MRA will have to be evaluated in comparison to the gold-standard digital subtraction angiography or high-resolution CE-MRA.

In conclusion, accelerated time resolved CE-MRA with imaging acceleration along the spatial encoding direction and temporal domain with a large field-of-view has shown applicable in routine clinical studies of the neurovascular and thoracic vasculature providing good to excellent arterial and venous image quality with additional information on pathologies derived from the given temporal update rate. Further comparative studies to the gold standard are warranted to reveal its accuracy.

References

1. Prince MR (1998) Peripheral vascular MR angiography: the time has come. Radiology 206:592–593
2. Korosec FR, Frayne R, Grist TM, Mistretta CA (1996) Time-resolved contrast-enhanced 3D MR angiography. Magn Reson Med 36:345–51
3. Foo TK, Saranathan M, Prince MR, Chenevert TL (1997) Automated detection of bolus arrival and initiation of data acquisition in fast, three-dimensional, gadolinium-enhanced MR angiography. Radiology 203:275–280
4. Wilman AH, Riederer SJ (1997) Performance of an elliptical centric view order for signal enhancement and motion artifact suppression in breath-hold three-dimensional gradient echo imaging. Magn Reson Med 38:793–802
5. Wilman AH, Riederer SJ, King BF, Debbins JP, Rossman PJ, Ehman RL (1997) Fluoroscopically triggered contrast-enhanced three-dimensional MR angiography with elliptical centric view order: application to the renal arteries. Radiology 205:137–146
6. Meaney JF, Ridgway JP, Chakraverty S, Robertson I, Kessel D, Radjenovic A, Kouwenhoven M, Kassner A, Smith MA (1999) Stepping-table gadolinium-enhanced digital subtraction MR angiography of the aorta and lower extremity arteries: preliminary experience. Radiology 211:59–67
7. Fink C, Ley S, Kroeker R, Requardt M, Kauczor HU, Bock M (2005) Time-resolved contrast-enhanced three-dimensional magnetic resonance angiography of the chest: combination of parallel imaging with view sharing (TREAT). Invest Radiol 40:40–48

8. Norris DG (2003) High field human imaging. J Magn Reson Imaging 18:519–529
9. Lotz J, Doker R, Noeske R, Schuttert M, Felix R, Galanski M, Gutberlet M, Meyer GP (2005) In vitro validation of phase-contrast flow measurements at 3 T in comparison to 1.5 T: precision, accuracy, and signal-to-noise ratios. J Magn Reson Imaging 21:604–610
10. Griswold MA, Jakob PM, Heidemann RM, Nittka M, Jellus V, Wang J, Kiefer B, Haase A (2002) Generalized autocalibrating partially parallel acquisitions (GRAPPA). Magn Reson Med 47:1202–1210
11. Riederer SJ, Tasciyan T, Farzaneh F, Lee JN, Wright RC, Herfkens RJ (1988) MR fluoroscopy: technical feasibility. Magn Reson Med 8:1–15
12. Fink C, Puderbach M, Ley S, Zaporozhan J, Plathow C, Kauczor HU (2005) Time-resolved echo-shared parallel MRA of the lung: observer preference study of image quality in comparison with non-echo-shared sequences. Eur Radiol 15:2070–2074
13. Hu HH, Madhuranthakam AJ, Kruger DG, Glockner JF, Riederer SJ (2006) Combination of 2D sensitivity encoding and 2D partial Fourier techniques for improved acceleration in 3D contrast-enhanced MR angiography. Magn Reson Imaging 55:16–22
14. Fenchel M, Requardt M, Tomaschko K, Kramer U, Stauder NI, Naegele T, Schlemmer HP, Claussen CD, Miller S (2005) Whole-body MR angiography using a novel 32-receiving-channel MR system with surface coil technology: first clinical experience. J Magn Reson Imaging 21:596–603
15. Ruehm SG, Goyen M, Barkhausen J, Kroger K, Bosk S, Ladd ME, Debatin JF (2001) Rapid magnetic resonance angiography for detection of atherosclerosis. Lancet 357:1086–1091
16. Schoenberg SO, Bock M, Floemer F, Grau A, Williams DM, Laub G, Knopp MV (1999) High-resolution pulmonary arterio- and venography using multiple-bolus multiphase 3D-Gd-mRA. J Magn Reson Imaging 10:339–346
17. Goldfarb JW, Prasad PV, Griswold MA, Edelman RR (2000) Dynamic three-dimensional magnetic resonance abdominal angiography and perfusion: implementation and preliminary experience. J Magn Reson Imaging 11:201–207
18. Weiger M, Pruessmann KP, Kassner A, Roditi G, Lawton T, Reid A, Boesiger P (2000) Contrast-enhanced 3D MRA using SENSE. J Magn Reson Imaging 12;671–677
19. Ohno Y, Kawamitsu H, Higashino T, Takenaka D, Watanabe H, van Cauteren M, Fujii M, Hatabu H, Sugimura K (2003) Time-resolved contrast-enhanced pulmonary MR angiography using sensitivity encoding (SENSE). J Magn Reson Imaging 17:330–336
20. Mistretta CA, Grist TM, Korosec FR, Frayne R, Peters DC, Mazaheri Y, Carrol TJ (1998) 3D time-resolved contrast-enhanced MR DSA: advantages and tradeoffs. Magn Reson Med 40:571–581
21. Sueyoshi E, Sakamoto I, Matsuoka Y, Ogawa Y, Hayashi H, Hashmi R, Hayashi K (1999) Aortoiliac and lower extremity arteries: comparison of three-dimensional dynamic contrast-enhanced subtraction MR angiography and conventional angiography. Radiology 210:683–688
22. Schoenberg SO, Essig M, Hallscheidt P, Sharafuddin MJ, Stolpen AH, Knopp MV, Yuh WT (2002) Multiphase magnetic resonance angiography of the abdominal and pelvic arteries: results of a bicenter multireader analysis. Invest Radiol 37:20–28
23. Duran M, Schoenberg SO, Yuh WT, Knopp MV, van Kaick G, Essig M (2002) Cerebral arteriovenous malformations: morphologic evaluation by ultrashort 3D gadolinium-enhanced MR angiography. Eur Radiol 12:2957–2964
24. Du J, Carroll TJ, Brodsky E, Lu A, Grist TM, Mistretta CA, Block WF (2004) Contrast-enhanced peripheral magnetic resonance angiography using time-resolved vastly undersampled isotropic projection reconstruction. J Magn Reson Imaging 20:894–900
25. Schoenberg SO, Rieger J, Weber CH, Michaely HJ, Waggershauser T, Ittrich C, Dietrich O, Reiser MF (2005) High-spatial-resolution MR angiography of renal arteries with integrated parallel acquisitions: comparison with digital subtraction angiography and US. Radiology 235:687–698
26. Nael K, Michaely HJ, Villablanca P, Salamon N, Laub G, Finn JP (2006) Time-resolved contrast enhanced magnetic resonance angiography of the head and neck at 3.0 tesla: initial results. Invest Radiol 41:116–124
27. Pruessmann KP (2004) Parallel imaging at high field strength: synergies and joint potential. Top Magn Reson Imaging 15:237–244
28. Reeder SB, Wintersperger BJ, Dietrich O, Lanz T, Greiser A, Reiser MF, Glazer GM, Schoenberg SO (2005) Practical approaches to the evaluation of signal-to-noise ratio performance with parallel imaging: application with cardiac imaging and a 32-channel cardiac coil. Magn Reson Med 54:748–754
29. Pruessmann KP, Weiger M, Scheidegger MB, Boesiger P (1999) SENSE: sensitivity encoding for fast MRI. Magn Reson Med 42:952–962